



HAL
open science

An advanced control for a PM synchronous motor drive in power degraded mode

Olivier Bethoux, Eric Labouré, Éric Berthelot, Abdelfatah Kolli, Alexandre de
Bernardinis

► **To cite this version:**

Olivier Bethoux, Eric Labouré, Éric Berthelot, Abdelfatah Kolli, Alexandre de Bernardinis. An advanced control for a PM synchronous motor drive in power degraded mode. *Mathematics and Computers in Simulation*, 2019, 10.1016/j.matcom.2019.02.001 . hal-02051635

HAL Id: hal-02051635

<https://hal.science/hal-02051635v1>

Submitted on 27 Feb 2019

HAL is a multi-disciplinary open access archive for the deposit and dissemination of scientific research documents, whether they are published or not. The documents may come from teaching and research institutions in France or abroad, or from public or private research centers.

L'archive ouverte pluridisciplinaire **HAL**, est destinée au dépôt et à la diffusion de documents scientifiques de niveau recherche, publiés ou non, émanant des établissements d'enseignement et de recherche français ou étrangers, des laboratoires publics ou privés.

Accepted Manuscript

An advanced control for a PM synchronous motor drive in power degraded mode

Olivier Béthoux, Eric Labouré, Eric Berthelot, Abdelfatah Kolli, Alexandre De Bernardinis,

DOI: [10.1016/j.matcom.2019.02.001](https://doi.org/10.1016/j.matcom.2019.02.001)

Reference:

Publisher: ELSEVIER

To appear in: ***Mathematics and Computers in Simulation***

Received date: 15 January 2018

Revised date: 31 August 2018

Accepted date: 1 February 2019

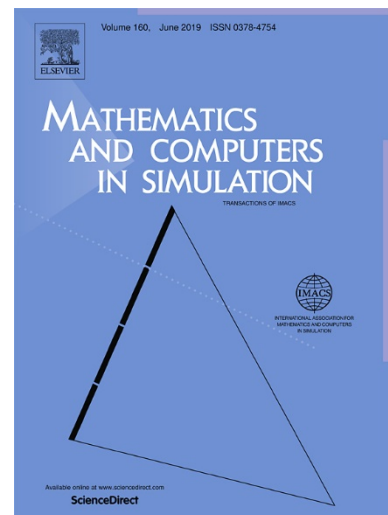
Date of Publication: 15 February 2019 (online)

To be published in (Volume XXX, Pages YY-ZZ)

Please cite this article as: O. Béthoux, E. Labouré, E. Berthelot, A. Kolli, A. De Bernardinis, An advanced control for a PM synchronous motor drive in power degraded mode, *Mathematics and Computers in Simulation*, 2019, ISSN 0378-4754, <https://doi.org/10.1016/j.matcom.2019.02.001>.

Document Version: Early version, also known as pre-print

This is a PDF file of an unedited manuscript that has been accepted for publication. As a service to our customers we are providing this early version of the manuscript. The manuscript will undergo copyediting, typesetting, and review of the resulting proof before it is published in its final form. Please note that during the production process errors may be discovered which could affect the content, and all legal disclaimers that apply to the journal pertain.



An Advanced Control for a PM Synchronous Motor Drive in Power Degraded Mode

O. Béthoux^{(1)*}, E. Labouré⁽¹⁾, E. Berthelot⁽¹⁾, A. Kolli⁽²⁾, A. De Bernardinis⁽²⁾

⁽¹⁾ GeePs | Group of electrical engineering – Paris, UMR CNRS 8507

Centralesupélec, Univ Paris-Sud, Sorbonne Universités, UPMC Univ Paris 06

3, 11 rue Joliot-Curie, Plateau de Moulon, F-91192 Gif-sur-Yvette CEDEX

⁽²⁾ SATIE (UMR 8029), IFSTTAR, CNRS, ENS Cachan, CNAM, Université Cergy-Pontoise,

F-78000 Versailles, France

* olivier.bethoux@centralesupelec.fr

CORRESPONDING AUTHOR: Olivier BETHOUX, Associate Professor, Univ Paris-Sud, France

AFFILIATION: GeePs | Group of electrical engineering – Paris

EMAIL: olivier.bethoux@centralesupelec.fr

TEL: +33(0)169851656

FAX: + 33(0)169418318

ABSTRACT

This paper deals with a control principle designed to allow remedial strategies for Permanent Magnet Synchronous Motor (PMSM) drives. The scope of the paper is focused on three-phase machines and it aims to present a simple and easy to tune control scheme for the system while it operates in degraded mode, namely when only two out of the three phases are operational. Compared to existing control strategy dedicated to degraded mode, this work proposes an

1 innovative one using new reference frames. Based on two innovative transformations applied
2 respectively to the currents and the voltages of the system, the proposed control scheme allows, in
3 degraded mode, the decoupling control of the states of the system and leads to continuous controller
4 references during system steady states. These properties lead to a very straightforward control
5 scheme based on independent PI controllers and to high static and dynamic performances. The
6 parameters setting of the controller is quite simple whatever the degree of magnetic coupling
7 between the two remaining motor phases. A laboratory test bench has been built to establish a proof
8 of concept of the suggested remedial strategy. It is based on a three-phase open-end-winding
9 permanent magnet machine fed with a power inverter made of three full H-bridge. This
10 experimental setup enables to validate the main operations of the ac motor drive under degraded
11 mode operation: torque control, speed change. Switching between healthy mode and faulty mode
12 is also performed successfully using this setup.

13

14 **KEYWORDS.**

15 Fault-tolerant control, control scheme, permanent-magnet synchronous motor (PMSM) drive,
16 phase loss, remedial strategy, availability.

17

18 **NOMENCLATURE.**

Symbol	Parameter
$[i_a \ i_b]^T$	real 3-phase machine winding currents in degraded mode
$[v_a \ v_b]^T$	real 3-phase machine winding voltages in degraded mode
L_a and L_b	self-inductances of the two remaining windings

M_{ab}	mutual inductance of the two remaining windings
R	Resistance of each winding
θ_e	rotor electrical angular position
ω_e	electric angular frequency
Ω	mechanic angular frequency
ε	magneto-motive force induced by the stator currents
x	considered angular position in the machine air gap
N_S	number of turns of the machine windings
T_i	two remaining currents transformation
T_v	two remaining voltages transformation
θ_{fr}	relative angular position of the fictitious frame to that of the rotor
$[i_\gamma i_\delta]^T$	fictitious 3-phase machine winding currents in degraded mode
$[v_\gamma v_\delta]^T$	fictitious 3-phase machine winding voltages in degraded mode
K_{SM}	speed constant of the fictitious machine
$[i_{\gamma,ref} i_{\delta,ref}]^T$	fictitious current references
K_p	coefficient for the proportional term of the PI controller
ω_I	coefficient for the integral term of the PI controller
H_k	transfer function of the current closed-loop

1 **Tab. 1. Nomenclature of the terms and symbols used in the document**

2

1 **1. INTRODUCTION**

2 Electric motor drives are often used for key functionalities which are mission critical and cannot
3 tolerate any unexpected periods of downtime due to a failure. Examples include many
4 manufacturing processes [1,2] and transport applications [3]. For instance power-assisted steering
5 of a ground vehicle [4, 5] or the actuators of the control surfaces of a plane [6] are key examples.
6 Some of these applications call for demanding specifications regarding high power density and
7 high efficiency. In such cases, the best choice is often a permanent magnet synchronous machine
8 [7]. This constraint is frequently associated with embedded systems and usually coincides with a
9 requirement for a high level of availability and reliability.

10 Several strategies can be successful in designing a fault-tolerant motor drive architecture. A first
11 example is increasing the number of converters either in parallel [8] or in series [9] as well as the
12 number of power switches using multicellular converters [10]. The second method that has been
13 explored is increasing the number of machines [11]. The third is using multiphase machines,
14 generally with an odd number of phases [12, 13]. These three methods are usually applied in high
15 power applications or products for which cost is not a key feature. However, the last solution can
16 also be used in low cost applications whilst permitting fault tolerant operation. For this purpose,
17 the lowest multiphase machine ($n = 3$) is the basic 3-phase motor. Two ways can be used to achieve
18 a fault-tolerant architecture: 1) using a 4-leg inverter and connecting the ac machine neutral point
19 to the fourth leg [14], [15], 2) using a 3-phase open-end-winding ac machine supplied by a power
20 inverter made of three full H-bridge [16], [17]. For example, the latter solution is proposed in the
21 car industry. It is covered by several patents owned by VALEO [18]-[21]; the overall system allows
22 achieving the three key power function of an electric vehicle, namely traction [22], fast and slow
23 charging [23], and grid assistance [24]. For this reason, the work covered here aims at designing a

1 proper control scheme, both simple and efficient to achieve the 2-phase operation mode of such a
2 3-phase synchronous machine.

3 Switching from a 3-phase to a 2-phase operation entails a structural change. In the 4-leg inverter
4 case, the phase currents sum is no longer equal to zero, in the open-winding case, the system
5 dimension decreases from three to two. To address this issue, S. Bolognani et al. computed the
6 optimal sinusoidal current reference for post fault operation [14]. They implemented this strategy
7 using a 4-leg inverter [15]. Their suggested fault-mode operation control scheme is based on the
8 Park fictitious machine. This leads to fictitious voltages with additional sinusoidal terms. As PI
9 controllers are not able to manage them properly, the control effectiveness is essentially based on
10 the cancellation of such terms. This indicates that this control scheme is primarily defined by the
11 precise knowledge of the motor parameters. Within the specific framework of a fully decoupled
12 synchronous machine, F. Baudart et al. calculate the optimal current references for any number of
13 motor phases [25]. In this specific case the current references track does not present any particular
14 difficulties since the system is structurally decoupled.

15 The aim of this article is to propose a unified approach enabling to design a control scheme for
16 achieving the real-time control of a 3-phase synchronous machine in 2-phase faulty mode. The
17 desired key points are: 1) simple to implement control scheme, 2) easy tuning of controllers
18 parameters, 3) constant control values delivered by the controllers in steady state, namely whilst
19 torque and speed are constant. The present work gives a clear insight of the theoretical basis related
20 to the proposed approach and goes on to its proof-of-concept in laboratory test bench trials.

21 This paper is organized as follows. The second section presents the fictitious machine related to
22 the aforementioned specifications. This leads to present the innovative transform matrices applied
23 to the electric values (e.g., currents and voltages). These transformations describe the link between

1 real and fictitious machines whose model will be presented in this part. The third section then
2 considers the appropriate control scheme of the two remaining phase currents and explains the
3 controller parameter setting method. The fourth section focuses on the experimental validation of
4 the suggested transformation concept and the related control scheme. The developed experimental
5 setup is described and trial results are presented and commented. This fully validates the ability of
6 the control scheme to maintain motor drive key functions during the application of the remedial
7 strategy as well as showing that switching from normal to faulty mode can be realized safely.
8 Finally, the last section draws conclusion and perspectives for future work.

9

10 **2. INNOVATIVE TRANSFORMATIONS AND FICTITIOUS MACHINE**

11 The present section addresses the control of only two phase currents of a 3-phase synchronous
12 machine. For clarity all notations are summarized in Tab. 1. An innovative set of transformations
13 is proposed in order to tackle this issue effectively. The aim is to design a fictitious machine (Fig. 1)
14 which

- 15 1) Produces the same magneto-motive force m.m.f. ε than the real machine but by the means
16 of two decoupled windings (these are being therefore orthogonal) fed by the fictitious
17 current $[i_\gamma \quad i_\delta]^T$;
- 18 2) Is driven by the fictitious voltage $[v_\gamma \quad v_\delta]^T$ enabling instantaneous power invariance;
- 19 3) Is supplied by constant variables during steady state (specifically while torque and rotational
20 speed are constant).

21 Note that it is considered here in an arbitrary manner that the faulty phase is the c-phase.

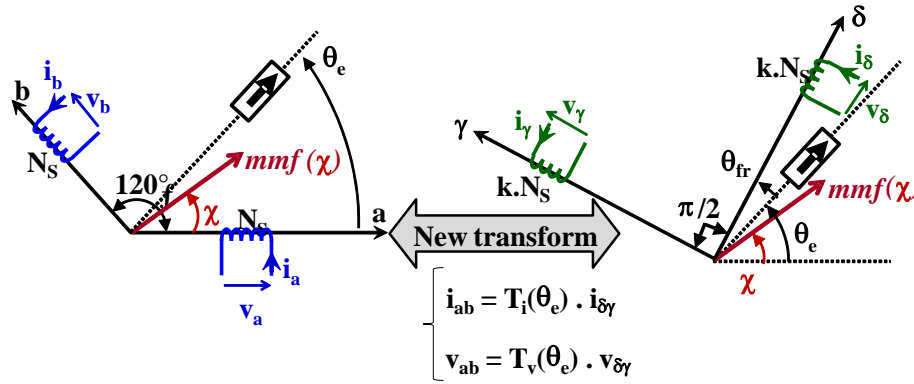


Fig. 1. Real and fictitious machines associated to innovative set of transformations.

To meet these three requirements, a set of two transformations T_i and T_v has to be defined. The first function is applied to the current and the second to the voltage. Obviously, the two mentioned functions depend on the rotor electrical angular position defined by $\theta_e(t)$.

$$\begin{bmatrix} i_a \\ i_b \end{bmatrix} = T_i(\theta_e) \begin{bmatrix} i_\delta \\ i_\gamma \end{bmatrix} \quad (1)$$

$$\begin{bmatrix} v_a \\ v_b \end{bmatrix} = T_v(\theta_e) \begin{bmatrix} v_\delta \\ v_\gamma \end{bmatrix} \quad (2)$$

With $[i_a \ i_b]^T$ and $[v_a \ v_b]^T$, the real machine current and voltage, respectively.

The θ_{fr} parameter described in Fig. 1 is a parameter which should be chosen to give the most convenient position of the new rotating frame. Likewise, the k parameter defines the voltage ratio between fictitious and real winding.

Based on the requirements, the three following subsections define the suggested transformation set. The fourth subsection derives the control-oriented model of the fictitious machine.

2.1. Power Invariance

To ensure that the two machines are equivalent, it is mandatory to ensure that the instantaneous power consumption of each machine are equal, as follows:

$$1 \quad \begin{bmatrix} v_a \\ v_b \end{bmatrix}^T \begin{bmatrix} i_a \\ i_b \end{bmatrix} = \begin{bmatrix} v_\delta \\ v_\gamma \end{bmatrix}^T T_v(\theta_e)^T T_i(\theta_e) \begin{bmatrix} i_\delta \\ i_\gamma \end{bmatrix} = \begin{bmatrix} v_\delta \\ v_\gamma \end{bmatrix}^T \begin{bmatrix} i_\delta \\ i_\gamma \end{bmatrix} \quad (3)$$

2 This mathematical equality implies the following relation between the two transfer matrix T_i and
 3 T_v :

$$4 \quad T_v(\theta_e)^T T_i(\theta_e) = Id \quad (4)$$

5 2.2. Remaining Currents Transformation

6 The m.m.f. ε_{real} of the real machine is expressed as a function of real currents. Noting x the angular
 7 position in the machine air gap, ε_{real} can be computed as:

$$8 \quad \varepsilon_{real} = AN_S [\cos(x) \quad \cos(x - 2\pi/3)] \begin{bmatrix} i_a \\ i_b \end{bmatrix} \quad (5)$$

9 With N_S the number of turns of the machine windings and A a machine geometry-dependent
 10 parameter.

11 To simplify motor drive control, it is useful to separate the two current components. This means,
 12 from a mathematical point of view, that the transformation must achieve the diagonalization of the
 13 inductance matrix $L_{ab}(\theta_e)$ defined by:

$$14 \quad L_{ab}(\theta_e) = \begin{bmatrix} L_a(\theta_e) & M_{ab}(\theta_e) \\ M_{ab}(\theta_e) & L_b(\theta_e) \end{bmatrix} \quad (6)$$

15 with L_a and L_b the self-inductances of the two remaining windings and M_{ab} their mutual
 16 inductance.

17 This first requirement involves the choice of two orthogonal fictitious winding, as depicted in
 18 Fig. 1. Equally, the requirement of having constant currents at steady state implies that the fictitious
 19 windings rotates synchronously with the rotor.

20 Using these preliminary findings, the second m.m.f. ε_{fict} is directly expressed in the new $\delta\gamma$ frame.

$$21 \quad \varepsilon_{fict} = AkN_S \left[\cos(x - \theta_e - \theta_{fr}) \quad \cos\left(x - \theta_e - \theta_{fr} - \frac{\pi}{2}\right) \right] \begin{bmatrix} i_\delta \\ i_\gamma \end{bmatrix} \quad (7)$$

1 The trigonometric identities help to simplify this expression:

$$2 \quad \varepsilon_{fict} = A \cdot k \cdot N_S \cdot [f_1(x) \quad f_2(x)] \cdot \begin{bmatrix} i_\delta \\ i_\gamma \end{bmatrix} \quad (8)$$

3 with f_1 and f_2 two functions of angle x and angle $\theta_e(t)$:

$$4 \quad \begin{cases} f_1(x) = \cos(x) \cdot \cos(\theta_e + \theta_{fr}) + \sin(x) \cdot \sin(\theta_e + \theta_{fr}) \\ f_2(x) = -\cos(x) \cdot \sin(\theta_e + \theta_{fr}) + \sin(x) \cdot \cos(\theta_e + \theta_{fr}) \end{cases} \quad (9)$$

5 At a general level, the transformation matrix T_i is characterized by four entries (a , b , c and d):

$$6 \quad T_i(\theta_e) = \begin{bmatrix} a & b \\ c & d \end{bmatrix} \quad (10)$$

7 Using T_i definition (1), the m.m.f. of the real machine ε_{real} is expressed as a function of the
 8 fictitious currents:

$$9 \quad \varepsilon_{real} = AN_S [\cos(x) \quad \cos(x - 2\pi/3)] \begin{bmatrix} a & b \\ c & d \end{bmatrix} \begin{bmatrix} i_\delta \\ i_\gamma \end{bmatrix} \quad (11)$$

10 Using trigonometric identities yields the final expression:

$$11 \quad \varepsilon_{real} = AN_S [g_1(x) \quad g_2(x)] \begin{bmatrix} i_\delta \\ i_\gamma \end{bmatrix} \quad (12)$$

12 With g_1 and g_2 determined by angle x and angle $\theta_e(t)$:

$$13 \quad \begin{cases} g_1(x) = \cos(x) \cdot (a - c/2) + \sin(x) \cdot (c \cdot \sqrt{3}/2) \\ g_2(x) = \cos(x) \cdot (b - d/2) + \sin(x) \cdot (d \cdot \sqrt{3}/2) \end{cases} \quad (13)$$

14 The identification of the four relevant parameters is obtained by equating both expressions of
 15 m.m.f. (8) and (12) whatever the position in the air gap ($0 \leq x \leq 2\pi$) and the two components of
 16 the fictitious current. This comparison leads to a system of four nonlinear equations involving the
 17 four listed parameters: a , b , c and d .

18

$$1 \quad \begin{cases} a - c/2 = k \cos(\theta_e + \theta_{fr}) \\ c \cdot \sqrt{3}/2 = k \sin(\theta_e + \theta_{fr}) \\ b - d/2 = -k \sin(\theta_e + \theta_{fr}) \\ d \cdot \sqrt{3}/2 = k \cos(\theta_e + \theta_{fr}) \end{cases} \quad (14)$$

2 Deciding arbitrarily that the real machine and the fictitious one have the same number of turns ($k =$
 3 1), (14) allows to derive the current transformation matrix:

$$4 \quad T_i(\theta_e) = \frac{2}{\sqrt{3}} \begin{bmatrix} \cos(\theta_e + \theta_{fr} - \pi/6) & -\sin(\theta_e + \theta_{fr} - \pi/6) \\ \sin(\theta_e + \theta_{fr}) & \cos(\theta_e + \theta_{fr}) \end{bmatrix} \quad (15)$$

5 Unlike the Concordia or Park transformations, it is important to note that this matrix is non-
 6 orthogonal. Indeed the inverse matrix of the matrix T_i is:

$$7 \quad T_i^{-1} = \begin{bmatrix} \cos(\theta_e + \theta_{fr}) & \sin(\theta_e + \theta_{fr} - \pi/6) \\ -\sin(\theta_e + \theta_{fr}) & \cos(\theta_e + \theta_{fr} - \pi/6) \end{bmatrix} \neq T_i^T \quad (16)$$

8 This is because instantaneous power invariance does not impose this constraint for a 3-phase ac
 9 machine when working only with two phases as shown in (4).

10 The θ_{fr} parameter is chosen by allocating a specific role to each fictitious winding. For instance, a
 11 wise choice consists in using i_δ current for adjusting the machine magnetization and i_γ for
 12 controlling the electromagnetic torque T_{em} . This is obtained by imposing θ_{fr} equal to zero. Doing
 13 so and adopting $i_{\delta\gamma}^T = [0 \quad T_{em}/(K_{SM} \cdot \sqrt{2})]^T$ for the fictitious currents, the real currents $[i_a \quad i_b]^T$
 14 are calculated from (1) and (16).

$$15 \quad \begin{bmatrix} i_a \\ i_b \end{bmatrix} = -\frac{T_{em}}{K_{SM} \cdot \sqrt{3}} \sqrt{2} \begin{bmatrix} \sin(\theta_e - \pi/6) \\ \sin(\theta_e - \pi/2) \end{bmatrix} \quad (17)$$

16 Where K_{SM} is the motor electromotive force constant defined by $K_{SM} = E/\Omega$.

17 Obviously (17) is similar to optimal sinusoidal current reference determined by [14]. Hence the
 18 first transformation T_i is well defined and the self-control current reference is also found in this

1 unified approach. The second step is to compute the voltage allowing to achieve these currents. To
 2 do so, the next subsection exhibits the voltage transformation T_v .

3 2.3. Voltage Transformation

4 As mentioned before, ensuring the power invariance imposes a constraint on voltage
 5 transformation matrix. Within the $\delta\gamma$ frame with $\varphi = 0$, and using (4), T_v matrix is expressed as:

$$6 \quad T_v = (T_i^{-1})^T = \begin{bmatrix} \cos(\theta_e) & -\sin(\theta_e) \\ \sin(\theta_e - \pi/6) & \cos(\theta_e - \pi/6) \end{bmatrix} \quad (18)$$

7 Considering the case of a sinusoidal back electromotive force $e_{ab} = [e_a \ e_b]^T$

$$8 \quad \begin{bmatrix} e_a \\ e_b \end{bmatrix} = -K_{SM}\sqrt{2} \left(\frac{1}{p} \cdot \frac{d\theta_e}{dt} \right) \begin{bmatrix} \sin(\theta_e) \\ \sin(\theta_e - 2\pi/3) \end{bmatrix} \quad (19)$$

9 The fictitious expression of back electromotive force $e_{\delta\gamma} = [e_\delta \ e_\gamma]^T$ can then be derived:

$$10 \quad \begin{bmatrix} e_\delta \\ e_\gamma \end{bmatrix} = K_{SM} \cdot \sqrt{2} \cdot \left(\frac{1}{p} \cdot \frac{d\theta_e}{dt} \right) \cdot \begin{bmatrix} 0 \\ 1 \end{bmatrix} \quad (20)$$

11 This is obviously a constant vector with a zero δ component and a γ component with the same
 12 magnitude than the real back electromotive force. The result is consistent with the expectations on
 13 this transformation. The next stage therefore consists in deriving the control-oriented model of the
 14 fictitious machine.

15 2.4. Fictitious Machine Model

16 In degraded mode operation i.e. with two out of three windings operating the real machine is
 17 described by a 2-dimensional equation system:

$$18 \quad \begin{bmatrix} v_a \\ v_b \end{bmatrix} = L_{ab} \frac{d}{dt} \begin{bmatrix} i_a \\ i_b \end{bmatrix} + R \begin{bmatrix} i_a \\ i_b \end{bmatrix} + \begin{bmatrix} e_a \\ e_b \end{bmatrix} \quad (21)$$

19 Using the two suggested transformation matrix T_i and T_v yields the fictitious machine model:

$$20 \quad \begin{bmatrix} v_\delta \\ v_\gamma \end{bmatrix} = T_v^{-1} L_{ab} T_i \frac{d}{dt} \begin{bmatrix} i_\delta \\ i_\gamma \end{bmatrix} + T_v^{-1} L_{ab} \omega_e \frac{dT_i}{d\theta_e} \begin{bmatrix} i_\delta \\ i_\gamma \end{bmatrix}$$

$$1 \quad +RT_v^{-1}T_i \begin{bmatrix} i_\delta \\ i_\gamma \end{bmatrix} + \begin{bmatrix} e_\delta \\ e_\gamma \end{bmatrix} \quad (22)$$

2 Where $\omega_e = d\theta_e/dt$ is the rotor electrical angular frequency.

3 As explained above, the last term is the back electromotive force defined in the previous
 4 paragraph. The penultimate term refers to the ohmic losses. Estimating the matrix product $T_v^{-1}T_i$
 5 shows that this expression re-introduces a coupling between δ and γ channels. However, the
 6 fictitious ohmic voltage can be easily cancelled using feed-forward terms based on current
 7 measurement and rotor angular position.

$$8 \quad T_v^{-1}T_i = \frac{2}{3} \begin{bmatrix} 2(\sin^2(\theta_e) + \sin^2(\theta_e + \pi/3)) & \cos(2\theta_e + \pi/6) + \sin(2\theta_e) \\ \cos(2\theta_e + \pi/6) + \sin(2\theta_e) & 2(\cos^2(\theta_e) + \cos^2(\theta_e + \pi/3)) \end{bmatrix} \quad (23)$$

9 The first two terms require the knowledge of the motor inductance matrix $L_{ab}(\theta_e)$. For example,
 10 in the case of a non-salient pole rotor, the three characteristic parameters are constant. In particular,
 11 with respect to a well-coupled stator windings, the mutual inductance M depends on the winding
 12 self-inductance $L = L_a = L_b$ and is expressed as:

$$13 \quad M = -L/2 \quad (24)$$

14 Consequently the fictitious inductance matrix $L_{\delta\gamma}$ is diagonal and has constant entries:

$$15 \quad L_{\delta\gamma} = T_v(\theta_e)^{-1}L_{ab}T_i(\theta_e) = \begin{bmatrix} L & 0 \\ 0 & L \end{bmatrix} \quad (25)$$

16 The second term, which is proportional to rotor speed Ω and can be hence likened to a back
 17 electromotive force, is characterized by an anti-diagonal matrix with constant parameters:

$$18 \quad L_{ab}\omega_e T_v(\theta_e)^{-1} \cdot \frac{dT_i(\theta_e)}{d\theta_e} = \begin{bmatrix} 0 & -L \\ +L & 0 \end{bmatrix} \cdot \omega_e \quad (26)$$

19 Finally, the model of a non-salient pole synchronous machine is fully consistent with the initial
 20 objectives. Indeed the last three terms of the related fictitious model can be offset by feedforward
 21 technique:

$$\begin{aligned} 1 \quad \begin{bmatrix} v_\delta \\ v_\gamma \end{bmatrix} &= \begin{bmatrix} L & 0 \\ 0 & L \end{bmatrix} \frac{d}{dt} \begin{bmatrix} i_\delta \\ i_\gamma \end{bmatrix} + \begin{bmatrix} 0 & -L \\ +L & 0 \end{bmatrix} \omega_e \begin{bmatrix} i_\delta \\ i_\gamma \end{bmatrix} \\ 2 \quad &+ R_{\delta\gamma} \begin{bmatrix} i_\delta \\ i_\gamma \end{bmatrix} + K_{SM} \Omega \sqrt{2} \begin{bmatrix} 0 \\ 1 \end{bmatrix} \quad (27) \end{aligned}$$

3

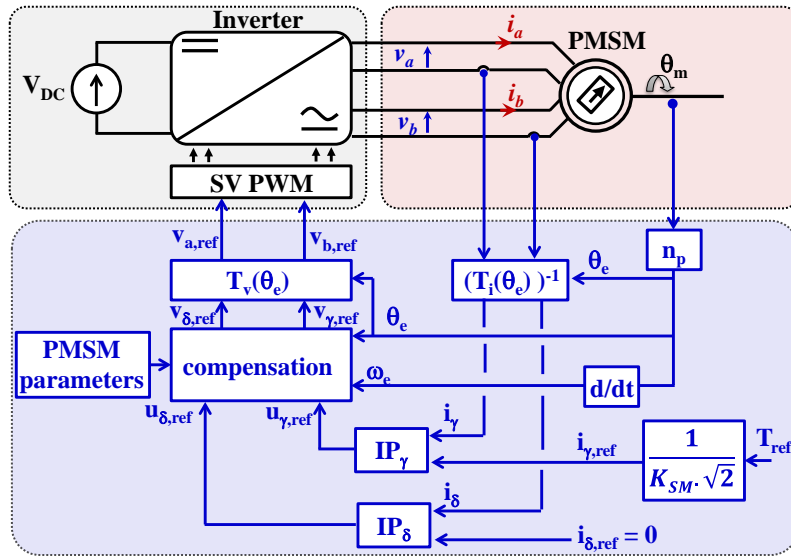
4 **3. CONTROL SCHEME IN DEGRADED OPERATION MODE**

5 The proposed fictitious machine related to the suggested transformation set is made of two
 6 orthogonal winding. The i_δ current in the first winding permits the adjustment of the air gap
 7 magnetic field whereas the i_γ current allows the control of the electromagnetic torque. Control
 8 variables are the two components of $[v_\gamma \ v_\delta]^T$ i. e., the voltages at the terminals of each motor
 9 winding. The latter are set up by a voltage inverter powered by a DC bus. To ensure a definite
 10 decoupling of the two fictitious windings, the control scheme must simply offset the coupling terms
 11 which means providing the three feed-forward compensation terms considered in the previous
 12 paragraph (Fig. 2). By doing so the fictitious machine is simply described by a set of two
 13 independent first order linear differential equations.

$$14 \quad \begin{bmatrix} u_\delta \\ u_\gamma \end{bmatrix} = \begin{bmatrix} L & 0 \\ 0 & L \end{bmatrix} \frac{d}{dt} \begin{bmatrix} i_\delta \\ i_\gamma \end{bmatrix} \quad (28)$$

15 Where $[u_\gamma \ u_\delta]^t$ is the new control command of the decoupled fictitious machine:

$$16 \quad \begin{bmatrix} v_\delta \\ v_\gamma \end{bmatrix} = \begin{bmatrix} u_\delta \\ u_\gamma \end{bmatrix} + \begin{bmatrix} 0 & -L \\ +L & 0 \end{bmatrix} \omega_e \begin{bmatrix} i_\delta \\ i_\gamma \end{bmatrix} + R_{\delta\gamma} \begin{bmatrix} i_\delta \\ i_\gamma \end{bmatrix} + K_{SM} \Omega \sqrt{2} \begin{bmatrix} 0 \\ 1 \end{bmatrix} \quad (29)$$



1
2
3
4
5
6
7
8
9
10
11

Fig. 2. Control scheme of the synchronous machine in remedial strategy.

3.1. Control Design

The controller parameters can be adjusted by classic control techniques such as Bode loop shaping or the root locus method [26]. Note that both subsystems have the same first-order dynamic behavior. Hence the decoupled system can be successfully controlled by two IP controllers with similar parameters. Using Laplace domain they are described by the following relations:

$$\begin{cases} u_{\delta} = K_P[-i_{\delta} + (i_{\delta,ref} - i_{\delta}) \omega_I/s] \\ u_{\gamma} = K_P[-i_{\gamma} + (i_{\gamma,ref} - i_{\gamma}) \omega_I/s] \end{cases} \quad (30)$$

The transfer function $H_k(s)$ between each current reference and the related current is a second-order lowpass filter whose parameters are the damping ratio m and the natural frequency ω_0 :

$$\begin{aligned} H_k(s) &= \frac{i_k(s)}{i_{k,ref}(s)} \\ &= \frac{1}{1 + s/\omega_I + s^2/(K_P\omega_I/L)} \\ &= \frac{1}{1 + 2ms/\omega_0 + s^2/\omega_0^2} \end{aligned} \quad (31)$$

1 To avoid current overshoot, the desired damping ratio is settled to $m = 1$. The dynamic response
2 of the control loop is tuned to get a closed-loop time response of about ten to twenty times the
3 switching periods leading to $F_0 = F_{SW}/20 = 1 \text{ kHz}$. These considerations induce the following
4 parameters adjustment:

$$\omega_I = \omega_0/2m = 3.15 \text{ krad. s}^{-1} \quad (32)$$

$$K_P = 2mL\omega_0 = 163.4 \text{ V. A}^{-1} \quad (33)$$

5 Additionally, an anti-windup compensator [27] acts on the integral term while the demanded
6 inverter output voltage is saturated by the DC bus supply; it may occur following a large current
7 reference change.

8 3.2. Control Strategy Sensitivity Analysis

9 It is critical to know in what manner and to what extent the performance of the suggested method
10 is sensitive to the change in the motor parameters. Indeed, they could evolve over time due to
11 internal machine temperature change or large stator current value.

12 Internal machine temperature may modify the B-H magnet characteristic, hence decreasing the
13 emf while the temperature increases. As stated before, it is important to underline that the emf
14 feedforward term is a constant. Hence an imprecise emf value does not affect the drive performance
15 as the controller integral term can easily offset it. This also applies to the slow changes due to
16 temperature fluctuations.

1 It is also necessary to consider a decrease in the inductance value due to machine magnetic
2 saturation whilst the motor operates at high current. As previously, the IP controller can
3 counterbalance the imprecise inductive voltage compensation in steady state mode. It should also
4 be stressed that the dynamic decoupling is no longer ideal. However the IP controller can
5 successfully reject this disturbance. Indeed the transfer function between the γ -current reference
6 and the δ -current is a fourth-order bandwidth filter with high attenuation even at the resonant
7 frequency. Fig. 3 shows a simulation which proves that a 5A γ -reference value step leads to a
8 negligible 11 mA δ -current overshoot in the event of an inductance decrease of 50 %. Moreover,
9 the γ -current response has no overshoot since an inductance decrease induces an increase of the
10 close-loop damping ratio. The response time is slightly affected by this change because the natural
11 frequency of the closed loop is increased by this change.

12 3.3. Power Inverter and related PWM

13 The suggested control strategy is a generic approach that can be applied to any voltage inverter
14 feeding the two remaining phases of a faulty 3-phase motor. More specifically two alternative
15 candidates [28] are:

- 16 • The 3 H-bridge inverter where each H-bridge drives a motor phase (fig. 4);
- 17 • The 4-leg inverter whose additional leg is connected to the motor neutral point and only
18 works in case of failure.

19 In the first case (Fig. 4), each phase is managed separately. Consequently the PWM scheme to
20 be used is the basic H-bridge PWM method which produces a 3-level output voltage.

21 In the second case, the neutral point voltage is common to each winding leading to a coupling of
22 both phase voltages. As a result the PWM scheme has to rely on a space vector approach [15], [16].

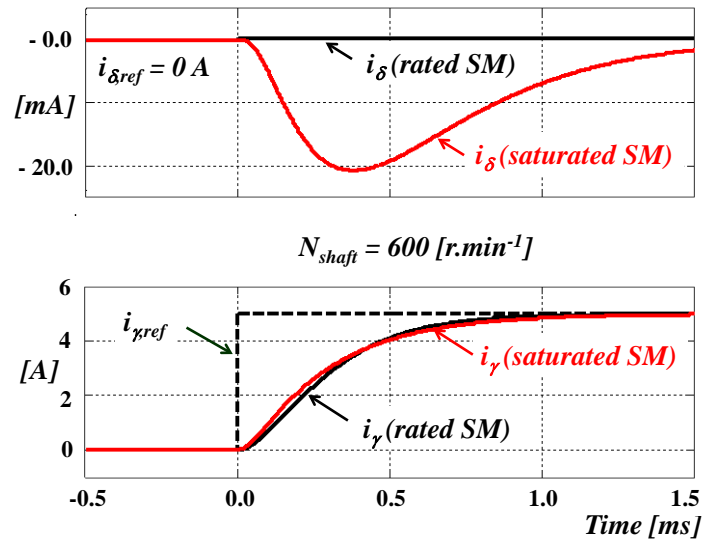


Fig. 3. Simulation of torque transient

under fault operation mode:

$N = 600 \text{ r.min}^{-1}$, $I_{\delta,ref} = 0 \text{ A}$ and $I_{\gamma,ref} = 0 \text{ A} \rightarrow 5 \text{ A}$.

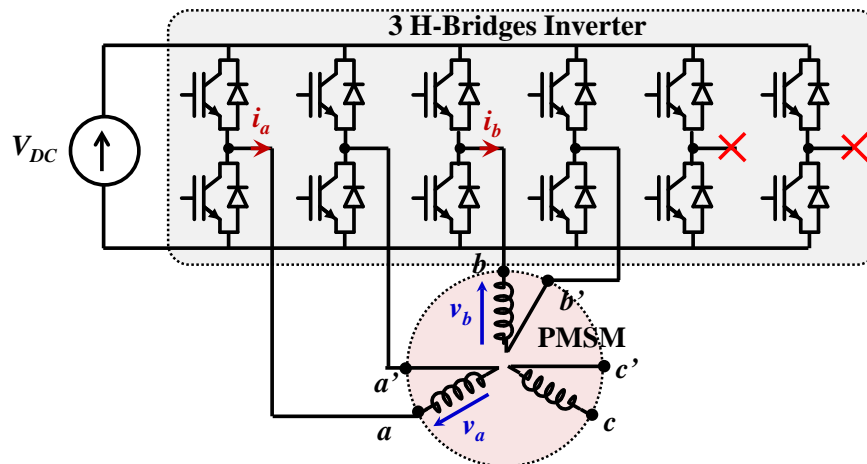


Fig. 4. Fault-tolerant architecture based on a 3 H-bridges inverter.

3.4. Project Framework

The drive requirement is to enable the continuity of service of the traction function when the electric vehicle is on the move. The purpose of the study is to allow the driver to reach an automobile repair shop in order to change the defective devices. This mission can be accomplished

1 at limited speed using a reduced torque range; this option limits any further failure in the motor
2 drive. That is the reason why current range for post fault operation is similar with the one for normal
3 mode. In addition, either in normal mode or in default mode operation, it could be interesting to
4 accurately monitor the dynamic friction in order to adjust the output torque reference [29]; such
5 supervision monitoring system could highly enhance the vehicle speed control at very low speed,
6 which would typically improve drivability during parking operation.

7 Furthermore the present work focuses on the post fault drive control strategy. It assumes that a
8 robust and effective fault detection and isolation (FDI) technique enables to detect the fault and
9 switch the system to its fault mode. Such technique could be successfully developed by combining
10 the fault tolerant method against current and speed sensor failure [30] and the FDI of phase and
11 switch faults [31].

12 Finally, the 3-phase motor in default mode operation has been studied and the proposed control
13 scheme defined. The next step is to validate experimentally the advantage of the suggested
14 approach.

15 **4. INNOVATIVE APPROACH PROOF OF CONCEPT**

16 4.1. Scale and scope of the contribution made

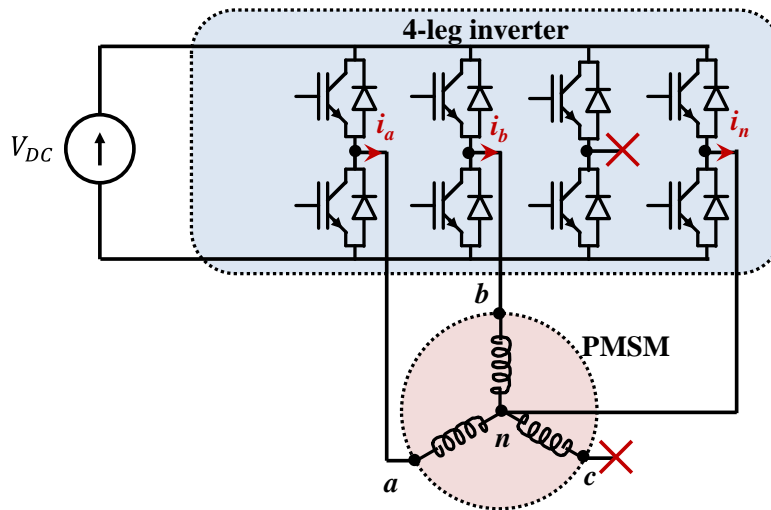
17 Before addressing the proof of the proposed concept, it seems important to stress the scale and
18 scope of the contribution made in order to place the present work within the context of previous
19 works around similar aspects.

20 One of the main value of the present proposal is that it offers a comprehensive approach of a
21 multiple input multiple output (MIMO) system based on the physical phenomena occurring in the
22 studied system, namely a 3-phase machine operating only with 2 out of its 3 windings. It hence
23 facilitates understanding and application of the approach by engineers in charge of developing AC

1 motor drives. Significantly, the benefits that electric drive developers may gain from this global
2 approach are numerous in terms of:

- 3 • Decoupling between the fictitious control actions (v_γ and v_δ) and (i_γ and i_δ) which
4 enables to design and tune simple PI controllers;
- 5 • Torque control which, in steady state, only requires to regulate constant currents. This
6 property is valuable, as it simplifies the current controller's specification: only the torque
7 dynamics response is to consider without taking rotor speed Ω into account. It is therefore
8 easy to meet the drive specifications.
- 9 • Implementation since the developed approach does not make any assumptions except the
10 linearity of magnetics phenomena which principle is commonly accepted regarding
11 motor drive control issues. Consequently, it enables to implement the proposed control
12 structure for any power architecture enabling remedial strategy (see figures 4 and 5),
13 namely
 - 14 ○ the 3 H-bridges inverter driving an open-end winding synchronous motor;
 - 15 ○ the 4-leg inverter driving a synchronous motor with a neutral point.

16 The assets described in the previous paragraph are the simple way to describe the payback that
17 can be achieved from the present contribution. These attractive results are mainly due to the use of
18 two different mathematical transformations (T_i and T_v), one dedicated to the currents, the other one
19 to the voltages. The related model remains convenient to use since the power invariance is fulfilled.



1
2 **Fig. 5. Fault-tolerant architecture based on a 4-leg inverter.**

3 The present proposal was preceded by various works on remedial strategies enabling AC drives
4 to keep working in the event of losing one of the motor winding. The authors were mainly focused
5 on designing dedicated AC machines and power architectures enabling normal and degraded modes
6 operation and on defining the degraded mode current references permitting a constant torque,
7 sometimes considering power losses minimization. The related implementations show that the
8 MIMO system must be controlled differently at the expense of a poorer reference tracking due to
9 disturbance terms, coupling terms or dynamic references.

10 S. Bolognani et al. [14, 15] suggest a control method purely dedicated to a 3-phase machine
11 supplied with a 4-leg inverter. They keep using the classic complete Park transform ($abc \rightarrow dq0$),
12 which induces to track a sinusoidal zero-current and use an additional inductance in series with the
13 neutral point because of the very small value of the zero sequence inductance.

14 Mohammad-Ali Shamsi-Nejad et al. [31] and Quntao An et al. [32] addresses the issue of both
15 the power architecture (3 H-bridge inverter versus 4-leg inverter) and current reference waveform
16 optimization. To implement a real-time control, they keep using the partial Park transform

1 (abc \rightarrow dq), which results in some torque fluctuations due to a poor current references tracking. On
2 the other hand, T. Labbé et al. [33] have clearly identified the inappropriateness of using the classic
3 Park transform. They tackle mathematically the control-oriented model issue basing their approach
4 on eigenvectors to diagonalize the machine model. In degraded mode operation, i.e. with two out
5 of three windings operating, the real machine is described by a 2-dimensional equation system:
6 they exhibit properly the two related eigenvectors and eigenvalues, but miss their decoupling goal
7 because applying a single transformation (based on eigenvectors) to both electrical variables, i.e.
8 currents and voltages. Specifically, the mutual inductance M_{ab} induces several harmonic terms
9 which can only be reduced but not canceled by tuning a parameter of the suggested transformation.
10 The simulation of the real-time control reveals significant fluctuations. Baudart et al. [25] address
11 the control issue of a general N -phase machine working with $(N - 1)$ windings only in the
12 hypothesis of a specific motor designed with zero coupling effect between the different polyphase-
13 motor windings. It permits the authors to achieve good control and focus on designing the optimal
14 references regarding Joule losses.

15 According to our best knowledge, although previous research has been extensive, the proposed
16 contribution gives a comprehensive and physics-based approach to address the design of an
17 efficient fault-tolerant control of a 3-phase machine operating in degraded mode operation i.e.
18 using only two out of three windings. Although the theoretical basis is the major contribution, it is
19 also more than important to put into practice the proposed concept for a reality check. That is the
20 goal of the two following sub-sections.

21 4.2. Experimental Test Bench

22 An experimental test bench (Fig. 6) has been developed to validate the innovative control
23 scheme. This enables the drive of the 3-phase machine in the default operation mode. This

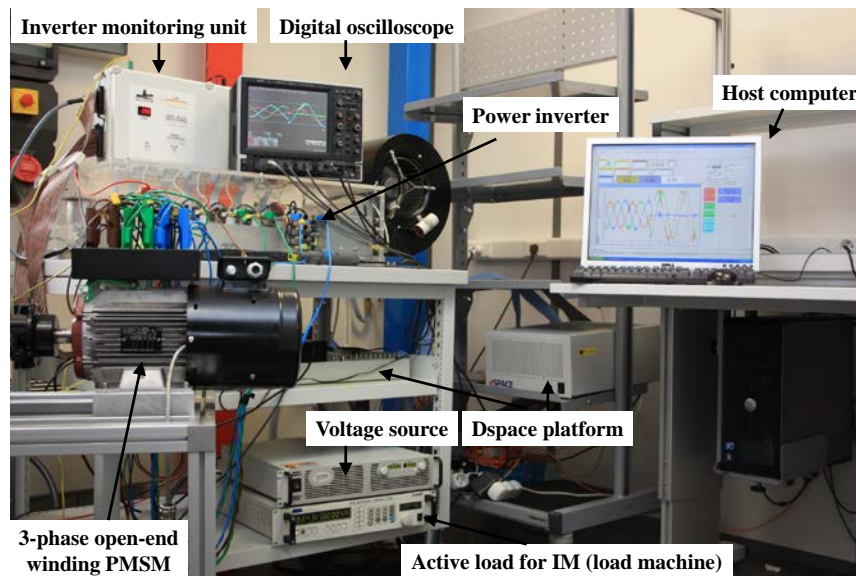
1 experimental setup (Fig. 7) is a two part interconnected system.

2 First, the system under test consists of

- 3 • A 3-phase open-end-winding permanent magnet synchronous machine (LEROY
4 SOMER) described in Tab. 2;
- 5 • An incremental encoder (IVO Industry) which provides rotor position data with a
6 resolution of 2500 points per revolution;
- 7 • An IGBT inverter made of six legs working at $F_{sw} = 20$ kHz switching frequency. In the
8 campaign's quantitative research trails, a leg is supposed faulty and hence both legs
9 driving the c winding are inhibited. Only 4 legs work to power the two remaining phases,
10 namely a and b ;
- 11 • A DC voltage source (AGILENT) supplies the DC bus with 300 V, 11 A rated voltage
12 and current, respectively. It is set to $V_{DC} = 300$ V;
- 13 • 2 Hall effect current sensors (LEM) for each motor winding characterized by a high
14 bandwidth (200 kHz) enabling to accurately measure the winding currents;

15 A real-time control system is built in a rapid prototyping technology system (designed by
16 DSPACE) around a two-level operating organization. It is organized around a DS1006 processor
17 board ensuring safety and reference management functions as well as the interface between the
18 daughter-boards or the host computer. The DS1006 card is connected with DS 3001 card which
19 permits to give absolute rotor position. It is also interconnected with DS5203 FPGA card equipped
20 with a FPGA Xilinx Virtex® 5 driven with a 100 MHz clock. The latter ensures inverter PWM
21 control signal generation (with a temporal resolution of 10 ns) as well as analogue-to-digital
22 conversion (based on a sampling time of $50 \mu s$ synchronized with the switching time T_{sw}). All
23 programs are developed using Matlab/Simulink software and then compiled and loaded into the

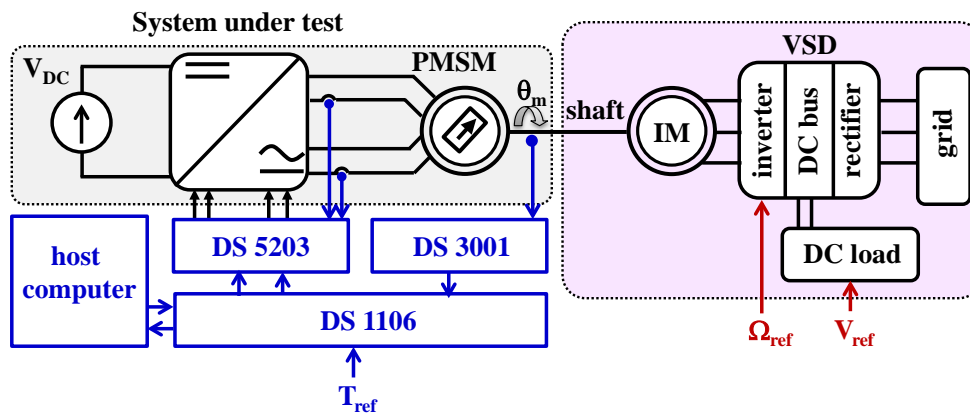
1 DSPACE system.



2

3

Fig. 6. Experimental setup view.



4

5

Fig. 7. Control scheme of the synchronous machine in remedial strategy.

6 As the machine under test is controlled with a torque reference, the second part of the test bench
 7 enables the control of the motor shaft rotation speed. It allows the emulation of the load system and
 8 hence the mimicking of real application behavior. This second component is composed of:

9

- A load induction machine (THRIGE ELECTRIC) with two pairs of poles;

10

- An industrial variable speed drive (OMRON);

- 1 • An AC 3-phase electric grid (400 V / 50 Hz);
 2 • A voltage-controlled active load (AMREL) with a 600 V voltage reference and connected
 3 to the DC stage of the load machine variable speed drive. It allows the recovery of any
 4 exceeding power provided by the machine under test.

5 Using this experimental setup several trials were undertaken and analyzed. They consist of
 6 operating the faulty machine in the steady state, the transient state as well as testing the ability of
 7 safely switching between healthy and faulty modes.

Symbol	Parameter	Value
R	Stator phase resistance	1.72 (Ω)
L_d	d-axis self-inductance	14 (mH)
L_q	q-axis self-inductance	12.5 (mH)
p	number of motor pole pairs	4
Ψ_M	amplitude of the induced flux	0.494 (Wb)
K_{SM}	Back-e.m.f. constant	1.417 (V s)
I_{rated}	Rated current	10 (A)

8 **Tab. 2. Leroy Somer LS 132 S synchronous motor parameters**

9 4.3. Analysis of Trial Results

10 1) Faulty steady state operation mode

11 To test the control scheme under steady state, the load machine is set at a constant speed, namely
 12 600 r.min⁻¹. The current reference is fixed at: $[i_{\delta,ref} \quad i_{\gamma,ref}]^T = [0 \text{ A} \quad 10 \text{ A}]^T$. The oscilloscope
 13 detects a trigger when the electric angle $\theta_e(t)$ passes through π value. Fig. 8 shows the related
 14 oscilloscope acquisition. Both real currents i_a and i_b are sinusoidal, have the same magnitude with
 15 60° phase shift and their phase offset regarding $\theta_e = \pi$ are $\pi/6$ and $\pi/2$, respectively. This

1 behavior is consistent with the relationship given in (16). Equally, the current frequency is 40 Hz
2 as expected with a synchronous machine with 4 pole pairs.

3 2) Torque transient

4 In order to assess the torque transient behavior, the second test is an i_γ current step response. The
5 motor shaft is still regulated at 600 r. min^{-1} and $i_{\delta,ref}$ is set at zero, whereas a 6.7 Hz pulse generator
6 delivers the i_γ current with two steps at 5 A and 15 A having the same duration. For this high
7 magnitude transient, the time response is small, i.e. about 1.8 ms, and the system signals do not
8 have any overshoot (Fig. 9).

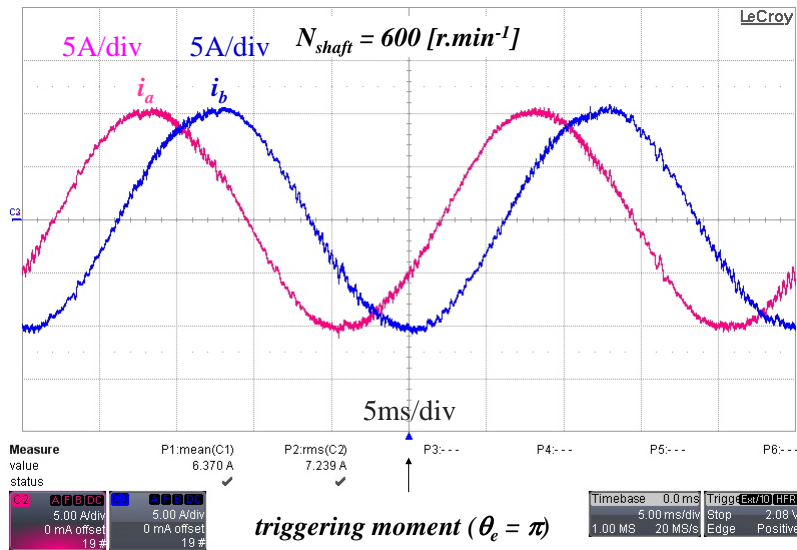
9 3) Speed transient

10 The motor current reference is kept constant at $[i_{\delta,ref} \quad i_{\gamma,ref}]^T = [0 \text{ A} \quad 10 \text{ A}]^T$ during the third
11 trial period. During this time, the load machine speed reference increases gradually from zero speed
12 to 600 r. min^{-1} with a slope of 0.04717 r.s^{-2} . The disturbance rejection is completely achieved since
13 the current magnitude is well regulated at 10 A throughout the transient period (Fig. 10).

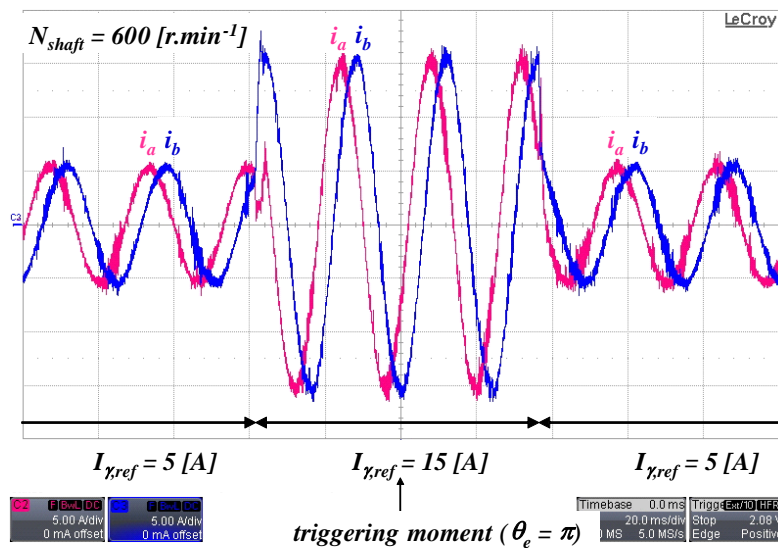
14 4) Switch from healthy to faulty mode operation

15 Finally it is crucial to assess the ability of the tested architecture to switch safely from a healthy
16 to a faulty operation mode. Several studies have already demonstrated that it is possible to diagnose
17 main faults on such ac drives without adding extra sensors [30]-[31], [35]. For this study it is hence
18 accepted that the inverter or motor default is rapidly detected and isolated. Hence, at $t = 0 \text{ s}$ (i.e. in
19 the middle of the oscilloscope screen) when the c-phase is inhibited in order to simulate an inverter
20 default, it is at the same moment the control scheme switches from the healthy to the faulty
21 algorithm. Despite the fault, the torque reference remains constant at 20 N.m. Fig. 11 shows that i_c
22 current falls to zero nearly instantaneously (driven by its own back electromotive force e_c).
23 Meanwhile, both the remaining currents rapidly modify their waveforms. Their phases change and

1 their magnitude increases by a factor $\sqrt{3}$ expanding by 7.1 A to 12.25 A. This test indicates that
 2 this architecture provides continuity of service for the driven application. This is a major asset for
 3 system reliability and it allows subsequent maintenance to be performed at a convenient place or
 4 moment.



6 **Fig. 8. Steady state default operation mode: $N = 600 \text{ r.min}^{-1}$, $I_{\delta,ref} = 0 \text{ A}$ and $I_{\gamma,ref} = 10 \text{ A}$.**



8 **Fig. 9. Torque transient under default operation mode: $N = 600 \text{ r.min}^{-1}$, $I_{\delta,ref} = 0 \text{ A}$ and**

9
$$I_{\gamma,ref} = 5 \text{ A} \leftrightarrow 15 \text{ A} .$$

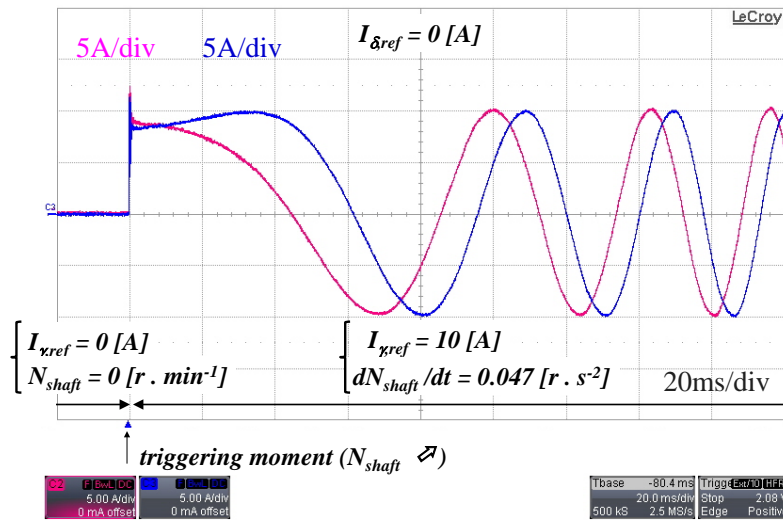


Fig. 10. Speed transient under default operation mode:

$N = 0 \rightarrow 600 \text{ r. min}^{-1}$, $I_{\delta,ref} = 0 \text{ A}$ and $I_{\gamma,ref} = 10 \text{ A}$.

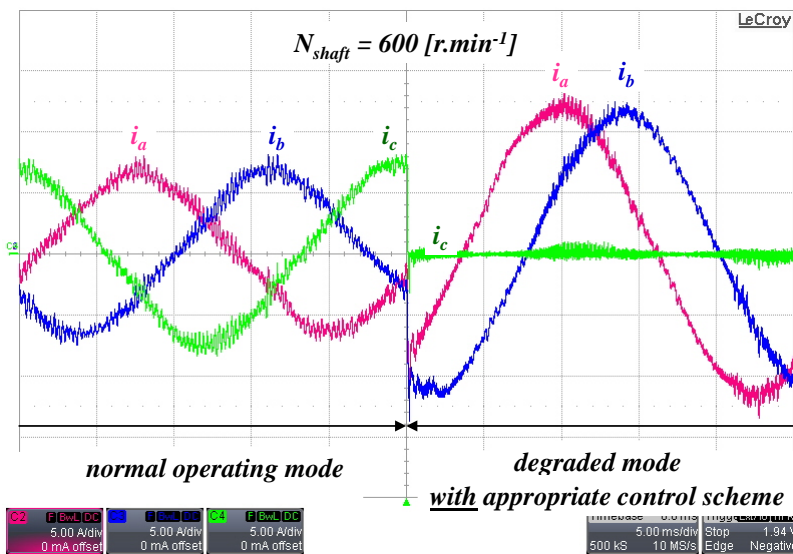


Fig. 11. A fault occurs on c-phase resulting in switching from normal to post-default control

scheme: $N = 600 \text{ r. min}^{-1}$ and $T_{ref} = 20 \text{ N m}$.

5. CONCLUSION AND PERSPECTIVES

This paper presents a remedial strategy for a fault in a 3-phase synchronous motor. Based on a 4-leg inverter or a 3 independent H-bridge inverter this basic machine is fault-tolerant to a single phase fault, which makes this architecture very attractive. The present work focuses on the

1 appropriate control scheme allowing to address the motor drive in faulty mode operation
2 adequately and efficiently. This is very important since continuity of service is a key factor of
3 modern drives.

4 The proposed method is based on an innovative voltage and current transformation set which
5 allows not only to decouple the remaining phase dynamics but also to control the electromagnetic
6 torque through constant current references in the steady state. These characteristics make it ideal
7 to use with two independent classic PI controllers. The latter are easy to tune using basic machine
8 parameters. In summary, this approach proposes a general framework for the problem and a
9 solution that is easy to implement.

10 A proof-of-concept of this theoretical approach has been established on a laboratory test bench
11 using a synchronous machine with 10 A rated current and an IGBT 3-H bridge inverter fed with a
12 300 V DC voltage source. The main motor drive features, namely torque tracking and speed
13 variation, have been successfully validated in degraded operation mode either at steady state or
14 transient state. In addition, in response to a detected default, the switching from healthy to faulty
15 control scheme was successfully tested. In conclusion the experimental results prove that the
16 proposed method gives attractive application prospects in terms of efficiency and simplicity of
17 implementation.

18 The formulation of the suggested fault-tolerant control strategies is wide-ranging and hence could
19 be extended to induction machine in further work. Another further work perspective is to deal with
20 the implementation of a flux-weakening strategy in the faulty mode operation.

21 **ACKNOWLEDGEMENT**

22 The authors gratefully acknowledge the French automotive cluster MOVEO for its financial
23 support through the SOFRACI project (in a FUI program).

1 **6. REFERENCES**

- 2 [1] Faa-Jeng Lin, Ying-Chih Hung, Jia-Ming Chen and Zi-Yin Kao, “Sensorless Inverter-Fed
3 Compressor Drive System Using Back-EMF Estimator with PIDNN Torque Observer”,
4 Asian J. Control, vol. 16, no. 4, pp. 1042–1056, July 2014.
- 5 [2] V. M. Hernández-Guzmán and J. Orrante-Sakanassi, “Global PID Control of Robot
6 Manipulators Equipped with PMSMs”, Vol. 20, No. 2, pp. 1–14, Mar. 2018
- 7 [3] Y. Song and B. Wang, “Survey on reliability of power electronic systems”, IEEE Trans.
8 Power Electron., vol. 28, no. 1, pp. 591–604, Jan. 2013.
- 9 [4] M. Naidu and S. Gopalakrishnan, “Fault-tolerant permanent magnet motor drive topologies
10 for automotive X-By-wire systems”, IEEE Trans. Ind. Appl., vol. 46, no. 2, pp. 841–848,
11 Mar./Apr. 2010.
- 12 [5] Sohail Anwar and Wei Niu, “A Nonlinear Observer Based Analytical Redundancy for
13 Predictive Fault Tolerant Control of a Steer-by-Wire System”, Asian J. Control, vol. 16,
14 no. 2, pp. 321–334, Mar. 2014.
- 15 [6] M. Villani, M. Tursini, G. Fabri, and L. Castellini, “High reliability permanent magnet
16 brushless motor drive for aircraft application,” IEEE Trans. Ind. Electron., vol. 59, no. 5,
17 pp. 591–604, May 2012.
- 18 [7] P.Sekerak, V. Hrabovcova, J. Pyrhonen, S. Kalamen, P. Rafajdus, M. Onufer, “Comparison
19 of Synchronous Motors With Different Permanent Magnet and Winding Types”, IEEE
20 Trans. Magn., Vol. 49, no. 3 , pp. 1256 - 1263, Mar. 2013.
- 21 [8] Z. Wang, J. Chen, M. Cheng, Y. Zheng, “Fault-Tolerant Control of Paralleled-Voltage-
22 Source-Inverter-Fed PMSM Drives,” IEEE Trans. Ind. Electron., Vol. 62, no. 8, pp. 4749 -
23 4760, Aug. 2015.

- 1 **[9]** A. Mora, P. Lezana, J. Juliet, “Control Scheme for an Induction Motor Fed by a Cascade
2 Multicell Converter Under Internal Fault”, *IEEE Trans. Ind. Electron.*, vol.61, no.11,
3 pp.5948-5955, Nov. 2014.
- 4 **[10]** P. Lezana, J. Pou, T.A. Meynard, J. Rodriguez, S. Ceballos, F. Richardeau, “Survey on
5 Fault Operation on Multilevel Inverters,” *IEEE Trans. Ind. Electron.*, Vol. 57, no. 7, pp.
6 2207 - 2218, July 2010.
- 7 **[11]** Chee-Shen Lim, E.Levi, M. Jones, N. Abd Rahim, Woi-Ping Hew, “A Fault-Tolerant
8 Two-Motor Drive With FCS-MP-Based Flux and Torque Control”, *IEEE Trans. Ind.*
9 *Electron.*, Vol. 61, no. 12, pp. 6603 - 6614, Dec. 2014.
- 10 **[12]** A. Tani, M. Mengoni, L. Zarri, G. Serra, D. Casadei, “Control of Multiphase Induction
11 Motors With an Odd Number of Phases Under Open-Circuit Phase Faults”, *IEEE Trans.*
12 *Power Electron.*, vol. 27, no. 2, pp. 565 - 577, Feb. 2012.
- 13 **[13]** Faa-Jeng Lin, Shih-Gang Chen and I-Fan Sun, “Adaptive Backstepping Control of Six-
14 Phase PMSM Using Functional Link Radial Basis Function Network Uncertainty
15 Observer”, *Asian J. Control*, Vol. 20, No. 1, pp. 1–15, Jan. 2018
- 16 **[14]** S. Bolognani, M. Zordan, M. Zigliotto, “Experimental fault-tolerant control of a PMSM
17 drive,” *IEEE Trans. Ind. Electron.*, Vol. 47, no. 5, pp. 1134 - 1141, Oct. 2000.
- 18 **[15]** N. Bianchi, S. Bolognani, M. Zigliotto, M. Zordan, “Innovative remedial strategies for
19 inverter faults in IPM synchronous motor drives”, *IEEE Trans. Energy Convers.*, Vol. 18,
20 no.2, pp. 306 - 314, June 2003.
- 21 **[16]** A. Kolli, O. Bethoux, A. De Bernardinis, E. Laboure, G. Coquery, “Space-Vector PWM
22 Control Synthesis for an H-Bridge Drive in Electric Vehicles,” *IEEE Trans. Veh. Technol.*,
23 Vol. 62, no. 6, pp. 2441 - 2452, July 2013.

- 1 [17] Yongjae Lee, Jung-Ik Ha, “Hybrid Modulation of Dual Inverter for Open-End Permanent
2 Magnet Synchronous Motor,” IEEE Trans. Power Electron., Vol. 49, no. 3 , pp. 1256 -
3 1263, June 2015.
- 4 [18] L. De Sousa and B. Bouchez, “Combined Electric Device for Powering and Charging”, US
5 Patent 20110221363 A1, Sept. 15, 2011.
- 6 [19] L. De Sousa and B. Bouchez, “Method and Electric Combined Device for Powering and
7 Charging with Compensation Means”, US Patent 20120019173 A1, Jan. 26, 2012.
- 8 [20] L. De Sousa, B. Bouchez, and J. L. Da Costa, “Method of exchanging electrical energy
9 between an electrical network conveying a dc or ac electrical quantity and an electrical
10 energy storage unit for hybrid or electric vehicle”, European Patent EP2794343 A2, Oct.
11 29, 2014.
- 12 [21] B. Bouchez and L. De Sousa, “Charge transfer device and associated management method”,
13 US Patent US20140042807 A1, Feb. 13, 2014.
- 14 [22] P. Sandulescu, F. Meinguet, X. Kestelyn, E. Semail, A. Bruyere, “Control Strategies for
15 Open-End Winding Drives Operating in the Flux-Weakening Region,” IEEE Trans. on
16 Power Electron., Vol. 29, no. 9, pp 4829 - 4842, Sept. 2014.
- 17 [23] S. Lacroix, E. Labouré, and M. Hilairet, “An integrated fast battery charger for electric
18 vehicle”, in Proc. VPPC 2010, 2000, Lille, pp. 1–6.
- 19 [24] N. Sakr, D. Sadarnac, A. Gascher, “A review of on-board integrated chargers for electric
20 vehicles”, in Proc. EPE'14-ECCE Europe, 2014, Lappeenranta, pp 1 - 10.
- 21 [25] F. Baudart, B. Dehez, E. Matagne, D. Telteu-Nedelcu, P. Alexandre, F. Labrique, “Torque
22 Control Strategy of Polyphase Permanent-Magnet Synchronous Machines With Minimal

- 1 Controller Reconfiguration Under Open-Circuit Fault of One Phase”, IEEE Trans. Ind.
2 Electron., Vol. 59, no. 6, pp. 2632 – 2644, June 2012.
- 3 **[26]** K. J. Astrom and T. Hagglund, “PID Controllers: Theory, Design, and Tuning,” 2nd edition,
4 Instrument Society of America (ISA), 1995.
- 5 **[27]** C. L. Hoo, Sallehuddin Mohamed Haris, Edwin C. Y. Chung and Nik Abdullah Nik
6 Mohamed, “New Integral Antiwindup Scheme for PI Motor Speed Control”, Asian J.
7 Control, vol. 17, no. 6, pp. 2115–2132, Nov. 2015.
- 8 **[28]** L. de Lillo, L. Empringham, P.W. Wheeler, S. Khwan-On, C. Gerada, and M. N. Othman,
9 “Multiphase power converter drive for fault-tolerant machine development in aerospace
10 applications”, IEEE Trans. Ind. Electron., Vol. 57, no. 2, pp. 575–583, Feb. 2010.
- 11 **[29]** Xingjian Wang, Shaoping Wang, “Output torque tracking control of direct-drive rotary
12 torque motor with dynamic friction compensation”, Journal of the Franklin Institute, Vol.
13 352, n° 11, pp. 5361-5379, Nov. 2015.
- 14 **[30]** C. Chakraborty, V. Verma, “Speed and Current Sensor Fault Detection and Isolation
15 Technique for Induction Motor Drive Using Axes Transformation”, IEEE Trans. Ind.
16 Electron, Vol. 62, no. 3, March 2015, pp. 1943 – 1954.
- 17 **[31]** F. Meinguet, P. Sandulescu, X. Kestelyn, E. Semail, “A Method for Fault Detection and
18 Isolation Based on the Processing of Multiple Diagnostic Indices: Application to Inverter
19 Faults in AC Drives”, IEEE Trans. Veh. Technol., vol.62, no.3, pp.995-1009, March 2013.
- 20 **[32]** M.-A. Shamsi-Nejad, B. Nahid-Mobarakeh, S. Pierfederici, F. Meibody-Tabar, “Series
21 architecture for fault tolerant PM drives: Operating modes with one or two DC voltage
22 source(s)”, Industrial Technology (ICIT), 2010 IEEE International Conference on, pp. 1525
23 - 1530, 2010.

- 1 [33] Quntao An, Guanglin Wang, Li Sun, “A fault-tolerant operation method of PMSM fed by
2 cascaded two-level inverters”, 7th International Power Electronics and Motion Control
3 Conference (IPEMC), vol. 2, pp. 1310 - 1313, 2012.
- 4 [34] T. Labbé, B. Dehez, and F. Labrique, “Two phase operation for a three phase PMSM using
5 a control model based on a Concordia like transform associated to a classic Park transform”,
6 Math. Comput. Simul., vol. 81, no. 2, pp. 315–326, Oct. 2010.
- 7 [35] Qun-Tao An; Li Sun; Li-Zhi Sun, “Current Residual Vector-Based Open-Switch Fault
8 Diagnosis of Inverters in PMSM Drive Systems”, IEEE Trans. Power Electron., Vol. 30,
9 no.5, pp.2814-2827, May 2015.
- 10